Designing an Open-Source Multi-vat Digital Light Processing Printer

Syed Raza ur Rehman [#1], Gene Tyler Felix [#1], Yuang Zhang[1], Akhilesh K Gaharwar[1,2,3]*

[1]Department of Biomedical Engineering, College of Engineering, Texas A&M University, College Station, TX 77843, USA
[2]Department of Material Science and Engineering, College of Engineering, Texas A&M University, College Station, TX 77843, USA
[3]Interdisiplinary program in Genetics and Genomics, Texas A&M University, College Station, TX 77843, USA
*Corresponding author E-mail: gaharwar@tamu.edu (A.K.G.)
[#]Equal contribution

Keywords: Digital Light Processing; Open Source; Multi-material; Additive Manufacturing

Abstract: Additive manufacturing has undergone rapid evolution in modalities that can recreate native human tissue architectures with high resolution. Among emerging approaches, digital light processing (DLP)-based printing enables the fabrication of intricate biomimetic architectures through the photopolymerization of polymer-based hydrogels. The recent emergence of multi-material printing further enhances this capability, enabling the complex spatial arrangement of heterogeneous cells and diverse bioink compositions. However, the widespread adoption of DLP printing remains constrained by the high cost, proprietary hardware, and limited customizability of commercially available systems. Here, we present an open-source multi-vat DLP printing platform developed through the integration and modification of two low-cost commercially available 3D printers. A dedicated Python-based graphical user interface was developed, providing user-defined control over critical printing parameters, including exposure time, layer height, printing sequence, and material switching. Comprehensive hardware documentation and a complete bill of materials (BOM) are provided to ensure reproducibility and accessibility across research laboratories. In addition to multi-material printing, the system enables spatial modulation of mechanical properties within a single bioink formulation through programmable light exposure and supports enhanced z-axis resolution through user-defined layer thickness control. The platform was validated through the fabrication of geometrically complex, multi-material, and mechanically heterogeneous constructs. Collectively, this work establishes an accessible and customizable DLP printing platform that enables advanced biofabrication and facilitates the engineering of compositionally and mechanically heterogeneous tissue-mimetic construct.

INTRODUCTION:

Additive manufacturing, also known as three-dimensional (3D) printing, has emerged as a powerful tool for the fabrication of biomimetic tissue constructs[1]. The growing demand for physiologically relevant *in vitro* models in tissue engineering, drug discovery, toxicology, and New Approach Methodologies (NAMs) has accelerated the development of advanced biofabrication technologies capable of recreating the structural and functional complexity of native tissues[2, 3]. Three-dimensional bioprinting enables the layer-by-layer assembly of biomaterials, cells, and bioactive factors into predefined geometries, providing unprecedented flexibility in the design of tissue-engineered constructs[4]. For polymeric materials, a diverse range of bioprinting techniques have been developed, including extrusion-based[5-8], inkjet-based[8, 9], laser-guided[9, 10], and light-based systems[11].

Among the various bioprinting modalities, light-based bioprinting techniques, particularly Digital Light Processing (DLP), have attracted significant attention due to their ability to rapidly fabricate high-resolution hydrogel constructs with excellent geometric fidelity[12]. Furthermore, the technology is compatible with a broad range of photocrosslinkable polymers, including gelatin, polyethylene glycol (PEG)[12-15], hyaluronic acid, and other bioactive hydrogel systems widely used in tissue engineering. Despite these advantages, most DLP systems are designed primarily for single-material fabrication, whereas native tissues are inherently heterogeneous in composition, cellular distribution, and mechanical properties[16, 17]. Although several research groups have reported the development of customized light-based bioprinting systems [11-15, 18], many of these platforms provide limited information regarding hardware design, system integration, software architecture, and fabrication workflows, thereby restricting reproducibility and broader adoption by the research community. For example, Wang et al. developed a low-cost stereolithography-based bioprinting system utilizing visible-light-crosslinkable bioinks [19], while Xiao et al. introduced a grayscale DLP printing approach capable of spatially tuning material properties [20]. However, the lack of comprehensive design documentation, open-source control software, and detailed assembly protocols often makes it challenging to reproduce, modify, or further develop these systems. Consequently, there remains a critical need for accessible, customizable, and fully documented DLP bioprinting platforms capable of fabricating both compositionally and mechanically heterogeneous tissue constructs.

To address the limited accessibility, high cost, and restricted customizability of commercial DLP bioprinting systems, we developed an open-source, multi-vat DLP bioprinting platform by integrating two low-cost commercial printers with open-source electronics and custom-designed mechanical components (**Figure 1A**). The system incorporates an automated rotary vat-switching mechanism and a custom Python-based control interface that enables multimaterial fabrication with reduced cross-contamination, user-defined layer thickness for improved z-axis resolution, and programmable stiffness patterning through controlled light exposure (**Figure 1B**). Complete design files, software resources, and a comprehensive bill of materials are provided to support reproducibility and community-driven development. The platform was validated by fabricating geometrically complex, multimaterial, and mechanically heterogeneous constructs, demonstrating an accessible and adaptable framework for advanced biofabrication, tissue engineering, and emerging NAMs applications.

MATERIALS AND METHODS

Hardware Assembly and System Integration

The open-source multi-vat DLP printer was constructed through the modification and integration of two commercially available desktop 3D printers: an Anycubic Photon Ultra resin printer and an Ender 3 Pro fused deposition modeling (FDM) printer. This approach was selected to maximize accessibility while minimizing system cost by reusing readily available hardware components. The Photon Ultra served as the foundation for the printing system due to its integrated NEMA 17 lead screw motor, linear guide rail,

and rigid metal projection module frame, all of which are well suited for DLP-based fabrication. Because the native control electronics and sensors of the Photon Ultra are proprietary, these components were replaced with open-source hardware to enable complete customization and software control.

Custom mechanical components were designed using computer-aided design (CAD) software and fabricated using a BambuLab A1 Mini printer with PLA filament (**Figure 2A**). The lead screw motor, metal chassis, and linear rail recovered from the Photon Ultra were mounted onto a metal optical breadboard using post holders and clamping forks to create the primary vertical motion assembly (**Figure 2B, Table 1**). The modular design allows similar components from alternative commercially available resin printers to be substituted, facilitating broader adoption and reproducibility.

The optical projection system was constructed using LightCrafter 4500 DLP projection modules (EKB Technologies) mounted onto Thorlabs optical carriers and linear rails (**Figure 2C-E**). The optical carriers enabled precise adjustment of the projector-to-build-plane distance to achieve accurate focusing at the projection plane. To further reduce the projected image area and improve printing resolution, the projector lens assembly was manually adjusted following removal of the factory-installed set screws. This configuration provided a flexible optical platform capable of accommodating different projection conditions and printing geometries.

To support automated multimaterial printing, a custom multi-vat platform was developed using a combination of recycled aluminum extrusion components from the Ender 3 Pro and RatRig V-Core 3 enclosure system together with custom-fabricated polymer components (**Figure 2F-I**). These components were assembled to create a rigid support structure upon which an acrylic sheet was mounted to serve as the transparent base for the rotating vat carousel. The carousel was designed to accommodate up to three independent resin vats and was driven by a stepper motor to enable automated material exchange during printing (**Figure 2F**). An optional enclosure fabricated from RatRig V-Core 3 panels was incorporated to provide environmental control and compatibility with external humidity regulation systems when required (**Figure 2I**).

To accommodate constructs of varying dimensions while minimizing resin consumption, interchangeable build platforms were developed using multiple substrate materials, including glass, acrylic, PLA, hook-and-loop fastener surfaces, and steel plates. These substrates were mounted onto a standardized printed base through adhesive or magnetic attachment methods (**Table 1**), enabling rapid customization of the build surface according to experimental requirements.

For resin containment, polystyrene petri dishes coated with polydimethylsiloxane (PDMS) were secured to the rotating carousel using a spring-loaded clamping mechanism consisting of custom clamps and retaining forks. The clamping system ensured consistent vat positioning during rotation while enabling rapid removal and replacement of individual vats. The final carousel assembly was capable of housing three separate resin vats for automated multimaterial fabrication.

System motion and automation were controlled using an SKR V1.4 Turbo controller board equipped with four TMC2209 stepper motor drivers and powered by a 12 V switching power supply (**Figure 2J-K**). Three independent stepper motors were used to control vertical platform movement, carousel rotation, and mechanical alignment operations. To ensure reproducible vat positioning during material switching, a dedicated alignment mechanism incorporating a movable mechanical end-stop switch was implemented. This system enabled accurate registration between the build platform and each resin vat, thereby minimizing positioning errors during multimaterial printing.

Software Development and Printer Control

To enable fully customizable printer operation and automated multimaterial fabrication, an open-source software framework was developed consisting of modified printer firmware and a custom Python-based

graphical user interface (GUI). The software architecture was designed to provide complete control over printer motion, material switching, exposure parameters, and slicing operations while maintaining compatibility with low-cost open-source hardware.

Printer motion and automation were controlled using an SKR V1.4 Turbo controller board equipped with TMC2209 stepper motor drivers. The controller operated using a customized version of Marlin 2.0 firmware obtained from the BigTreeTech repository and modified to accommodate the unique kinematic requirements of the multimaterial DLP bioprinter. Firmware modifications included optimization of motor microstepping, feed rates, homing procedures, positional limits, and real-time motion feedback to support accurate build platform positioning and automated rotary vat alignment. A complete description of firmware modifications and configuration parameters is provided in the Supporting Information.

A custom graphical user interface was developed in Python to coordinate printer operation and automate the fabrication workflow (**Figure S2**). The software enables user-defined control of critical printing parameters, including exposure time, layer thickness, printing sequence, material selection, and stiffness patterning. Communication between the software and controller board was achieved through standard serial communication protocols, allowing synchronized control of build platform motion, vat switching operations, and image projection.

To support multimaterial fabrication, a custom slicing pipeline was developed using the Trimesh and PySLM libraries. Unlike conventional resin-printing software packages that automatically reposition imported models within the build volume, the custom slicer preserves the original spatial coordinates of imported STL files. This functionality enables multiple independently designed components to be exported as separate STL files while maintaining their relative spatial positions within the final construct. As a result, different material compositions, exposure conditions, or mechanical properties can be assigned to specific regions of a construct without compromising geometric alignment.

The software workflow begins with the export of individual STL files corresponding to regions requiring distinct material compositions or exposure conditions. These files are imported into the custom GUI, where users assign printing parameters including exposure duration and resin-vat selection. The software subsequently generates layer-by-layer projection images and automatically coordinates build platform movement, projector operation, and rotary vat switching throughout the printing process. Prior to printing, the rotary stage is aligned using a mechanical end-stop positioning system to ensure accurate registration between the build platform and each resin vat. Once initialized, the fabrication process proceeds autonomously without additional user intervention.

Both the modified firmware and the custom Python software are distributed under an open-source license and are freely available through a public GitHub repository to facilitate reproducibility, customization, and future community-driven development.

Bioink preparation

A photocrosslinkable bioink formulation were prepared to evaluate the multimaterial and stiffness-patterning capabilities of the developed DLP bioprinting platform. The bioink consisted of 15% (w/v) polyethylene glycol diacrylate (PEGDA, Mn = 575 Da; Sigma-Aldrich) dissolved in phosphate-buffered saline (PBS) and supplemented with 15 mM lithium phenyl-2,4,6-trimethylbenzoylphosphinate (LAP) photoinitiator (LAP; CAS 85073-19-4; AmBeed, Cat. No. A636763) and 0.5 mM tartrazine photoabsorber (CAS 1934-21-0; TargetMol, Cat. No: TN2258). Bioink was prepared at room temperature and protected from ambient light prior to use.

For visualization of multimaterial printing and cross-contamination studies, PEGDA formulations were independently supplemented with either Rhodamine B (10 μg/mL) or methylene blue (10 μg/mL). These dyed formulations were used to evaluate material transfer during automated vat-switching operations.

Fabrication of Multimaterial and Stiffness-Patterned Constructs

Three-dimensional models were designed using Blender (Blender Foundation, Amsterdam, Netherlands) or SolidWorks (Dassault Systèmes, Waltham, MA, USA). For vascular channel constructs requiring support structures, automatic support generation was performed using Chitubox Basic prior to re-exporting the models as STL files. To preserve spatial registration during multimaterial fabrication, all STL files were exported without modifying their original coordinates and subsequently processed using the custom Python-based slicing software described previously.

All printing experiments were performed using the LightCrafter 4500 Mk II projection module operating at 405 nm with a measured intensity of 11 mW/cm^2 at the projection plane. For multimaterial fabrication, a layer thickness of 500 μm and an exposure time of 5 s per layer were used. The rotary vat carousel contained two bioink vats, one washing vat containing PBS, and one drying station containing a stationary absorbent foam. Following each material transition, the build platform was immersed in the PBS washing bath for 10 s and subsequently transferred to the drying station for 5 s to remove residual liquid prior to entering the next bioink vat. Additional dipping cycles were incorporated when necessary to eliminate trapped air bubbles and improve structural fidelity.

Cross-contamination between bioinks was evaluated using Rhodamine B- and methylene blue-labeled PEGDA formulations. Following multimaterial printing, residual bioinks were collected and analyzed using UV-visible spectroscopy. The absorbance of Rhodamine B at 580 nm was measured to quantify dye transfer between vats, and relative absorbance values were used to assess contamination before and after implementation of the washing and drying workflow.

To demonstrate programmable stiffness modulation using a single bioink formulation, PEGDA constructs were fabricated at a layer thickness of 10 μm using spatially controlled exposure times. Regions corresponding to soft tissue were exposed for 5 s per layer, whereas regions corresponding to bone were exposed for 15 s per layer. Mechanical properties were subsequently characterized by compression testing. The versatility of the platform was further demonstrated through the fabrication of vascular channels, gradient scaffolds, anatomical models, and bone-soft tissue interface constructs.

RESULTS AND DISCUSSION:

Design and Construction of the Open-Source Multi-Vat DLP Bioprinter

The open-source multi-vat DLP bioprinter was assembled by integrating low-cost commercial printer components with open-source electronics and custom-designed mechanical parts (**Figure 1A**). The modular architecture enabled automated vat switching during sequential printing while preserving user control over key fabrication parameters, including material exchange, layer thickness, and light exposure. This configuration supported multimaterial construct fabrication with limited material carryover between vats, improved z-axis control through adjustable layer thickness, and exposure-dependent modulation of hydrogel crosslinking to generate spatial variations in stiffness (**Figure 1B**). The design strategy emphasized functionality, accessibility, and adaptability by repurposing readily available components from consumer-grade 3D printers. In contrast to commercial DLP systems that often rely on proprietary hardware and software, this platform provides user access to hardware design files, control software, firmware configurations, and assembly procedures [7, 21, 22]. Together, these features establish a customizable DLP bioprinting workflow for fabricating compositionally and mechanically heterogeneous constructs.

The printer architecture consists of four primary subsystems: a DLP projection module, a motorized build platform, an automated rotary multi-vat mechanism, and a custom software control framework. Components recovered from an Anycubic Photon Ultra resin printer, including the lead screw assembly,

linear guide rail, and projection chassis, were repurposed to provide precise vertical positioning of the build platform. Open-source motion control was achieved using an SKR V1.4 Turbo controller board operating with a customized Marlin firmware configuration, eliminating dependence on proprietary electronics and enabling complete control over printer operation.

A key feature of the platform is the incorporation of a rotary multi-vat system capable of sequentially positioning multiple resin reservoirs above the projection plane. The carousel was designed to accommodate two bioink vats together with dedicated washing and drying stations, enabling automated multimaterial fabrication without manual intervention. In contrast to conventional vat-exchange workflows that require user interaction between printing steps, the automated switching mechanism allows rapid transitions between materials while maintaining alignment between successive layers. The integration of washing and drying stations further reduces residual material cross-contamination, a common challenge associated with multimaterial photopolymerization systems.

The optical subsystem was based on a LightCrafter 4500 Mk II projection module operating at 405 nm with a measured intensity of 11 mW/cm^2 at the printing plane. The projector was mounted on adjustable optical rails that enabled precise focal adjustment and customization of the projected image size. This modular configuration allowed the projection system to be optimized for both large-scale multimaterial constructs and high-resolution fabrication. Furthermore, user-defined layer thickness control was incorporated into the software architecture, enabling fabrication at layer heights as low as 1 μm for applications requiring enhanced z-axis resolution.

To provide flexible control over the printing process, a custom Python-based graphical user interface was developed to coordinate image projection, vat movement, material switching, and exposure control (**Figure S1**). Unlike conventional resin-printing software that assumes single-material fabrication, the custom software preserves the spatial registration of independently imported STL files, enabling distinct materials or exposure conditions to be assigned to specific regions within a construct. This capability provides a straightforward strategy for fabricating compositionally heterogeneous structures as well as mechanically heterogeneous constructs through spatial modulation of exposure parameters.

Collectively, the developed system combines automated multimaterial printing, programmable stiffness patterning, and tunable high-resolution fabrication within a fully documented open-source framework. These capabilities establish the foundation for the fabrication of compositionally and mechanically complex hydrogel constructs, which are evaluated in the subsequent sections.

Automated Multi-Material Fabrication and Cross-Contamination Mitigation

The incorporation of a rotary multi-vat mechanism enables the developed platform to fabricate heterogeneous constructs by sequentially exposing UV light to multiple photocrosslinkable bioinks during a single print job. To demonstrate this capability, a brain model was 3D printed using two independently dyed PEGDA formulations containing methylene blue and Rhodamine B, respectively (**Figure 3A-E**). Printing was performed using a 15% (w/v) PEGDA formulation supplemented with 15 mM LAP and 0.5 mM tartrazine, utilizing a layer height of 500 μm and an exposure time of 5 s per layer. The LightCrafter 4500 Mk II projector operating at 11 mW/cm^2 enabled rapid fabrication while the custom Python-based software automatically aligned, sliced, and assigned independently imported STL files to separate resin vats. The resulting construct demonstrated the ability of the platform to generate spatially heterogeneous structures without manual intervention between material exchanges.

Although multi-vat printing significantly expands the capabilities of DLP fabrication, residual resin transfer between vats can introduce cross-contamination and reduce interface fidelity [23]. Initial prints fabricated without intermediate cleaning exhibited visible color bleeding at material boundaries, indicating substantial material carryover during vat transitions. To address this challenge, dedicated washing and drying stations were incorporated into the printing workflow (**Figure 3F**). Following each

material transition, the build platform was immersed in a PBS washing bath and subsequently contacted with an absorbent foam drying station prior to entering the next resin vat. An additional dipping step was introduced after material exchange to remove trapped air bubbles and improve resin replenishment around the printed structure.

To determine the optimal contamination-mitigation strategy, five different workflows were evaluated: no washing/no drying (NWD), only washing (OW), only drying (OD), washing and drying (WD), and washing-drying with extra dipping cycles (WD+ED) (**Figure 4A**). UV-visible spectroscopy was performed on recovered resin samples following printing, and Rhodamine B absorbance at 580 nm was used as a quantitative indicator of resin carryover. Among all conditions tested, the WD+ED protocol consistently produced the lowest absorbance values, indicating the greatest reduction in cross-contamination. Correspondingly, ring, puzzle, and line models fabricated using the WD+ED workflow exhibited the highest interface fidelity and the least visible color mixing between adjacent regions (**Figure 4A & S1**).

The effects of printed layer number and build plate area on contamination were also systematically investigated (**Figure 4A & S1**). Increasing the number of printed layers from 1 to 8 progressively increased Rhodamine B transfer between vats, with absorbance values reaching approximately 0.13 arbitrary unit (AU) following an eight-layer print. This trend is likely attributable to the accumulation of uncured resin on the construct surface during repeated vat transitions. Incorporation of the washing and drying workflow reduced the absorbance to approximately 0.06 AU under equivalent printing conditions, corresponding to a greater than 50% reduction in contamination. Similarly, increasing the build plate size from 20 mm to 50 mm resulted in elevated dye transfer, suggesting that larger surface areas retain greater quantities of residual resin during material exchange. Under these conditions, contamination increased to approximately 0.085 AU in the absence of cleaning but was reduced to approximately 0.065 AU when washing and drying operations were employed.

The effectiveness of the optimized workflow was further validated through the fabrication of complex multimaterial geometries (**Figure 4B**). Distinct boundaries between the two resin formulations were clearly maintained across multiple printed architectures, demonstrating that the combination of automated vat switching, washing, drying, and bubble-removal steps enables reliable multimaterial DLP printing with minimal material carryover. Collectively, these results establish a practical strategy for mitigating one of the primary challenges associated with multi-vat photopolymerization systems and highlight the potential of the platform for fabricating compositionally heterogeneous tissue-engineered constructs.

High-Resolution Fabrication of Complex Hydrogel Architectures

The ability to fabricate geometrically complex structures with high fidelity is a critical requirement for tissue engineering and biofabrication applications [24]. While the lateral (x-y) resolution of DLP printing is largely governed by the optical characteristics of the projection system, the vertical (z-axis) resolution can be improved through precise control of layer thickness. Commercially available DLP bioprinters commonly restrict user control over minimum layer height, thereby limiting the fabrication of structures requiring fine vertical features. In contrast, the custom software developed in this work provides direct user control over layer thickness, enabling fabrication at significantly reduced layer heights for high-resolution applications.

To demonstrate the high-resolution capabilities of the platform, a nephron-inspired vascular construct was fabricated using a layer thickness of 5 μm and a projection intensity of 11 mW/cm^2 (**Figure 5A-B**). To maintain structural integrity during fabrication of the embedded vascular network, a formulation consisting of 20% (w/v) PEGDA, 40 mM LAP, and 2 mM tartrazine was utilized. The construct was successfully fabricated with perfusable channel features measuring approximately 1 mm in diameter,

and the printed geometry closely matched the original CAD design, demonstrating excellent dimensional fidelity. The enhanced resolution achieved through reduced layer thickness enabled accurate reproduction of the intricate looping architecture characteristic of nephron-inspired structures.

To further demonstrate the versatility of the platform, a variety of anatomically relevant and architecturally complex models were fabricated, including kidney, ear, stomach, finger, heart, truss, and gyroid structures (**Figure 5C**). These constructs contained intricate external and internal features that were successfully reproduced without structural collapse or loss of geometric detail. Notably, the heart model contained enclosed internal channels and hollow regions that remained intact following fabrication, highlighting the capability of the system to produce complex volumetric architectures. Collectively, these results demonstrate that the developed platform is capable of fabricating high-fidelity hydrogel structures spanning both engineered lattice geometries and anatomically inspired tissue models.

In addition to multimaterial fabrication, the developed platform enables spatial modulation of mechanical properties using a single bioink formulation through software-controlled variation of light exposure. Because photopolymerization kinetics directly influence crosslinking density, localized adjustment of exposure time provides a straightforward strategy for generating mechanically heterogeneous constructs without requiring multiple material formulations [25]. Such functionality is particularly attractive for tissue engineering applications, as many native tissues exhibit spatial variations in stiffness that influence cellular behavior and tissue function [26].

To demonstrate this capability, independently exported STL files corresponding to different regions of a construct were assigned distinct exposure conditions within the custom software environment. Regions representing compliant tissue were exposed for 5 s per layer, whereas mechanically stiffer regions were exposed for 15 s per layer using the same PEGDA formulation and projection intensity. Compression testing revealed that increasing exposure time produced a substantial increase in construct stiffness, with compressive modulus values increasing from approximately 50 kPa for the low-exposure condition to approximately 200 kPa for the high-exposure condition. This four-fold increase in stiffness was achieved without altering bioink composition, illustrating the ability of the platform to generate mechanically heterogeneous structures through software-defined fabrication parameters alone.

The spatial variation in crosslinking density was further visualized using methylene blue-containing formulations (**Figure 5D**). Methylene blue undergoes partial photobleaching when exposed to prolonged light doses, resulting in a visible reduction in color intensity with increasing exposure. Consequently, regions receiving greater light dosage appeared progressively lighter than regions exposed for shorter durations, providing a convenient visual indicator of stiffness patterning. Both discrete and continuous stiffness gradients were successfully generated across printed constructs, demonstrating precise spatial control over exposure dosage.

Limitations and Future Opportunities

While the developed open-source multi-vat DLP bioprinting platform demonstrates automated multimaterial fabrication, programmable stiffness patterning, and high-resolution printing, several limitations remain that present opportunities for future development. First, although the rotary system enables automated material switching, the current workflow introduces additional processing time due to the washing and drying steps required to minimize cross-contamination. Future optimization of the vat-switching mechanism, including automated fluid handling systems, or active washing modules could further improve fabrication efficiency while reducing cross-contamination.

Second, the exposure-based stiffness patterning offers a simple and efficient strategy for generating mechanical gradients, minor deviations between the designed and fabricated geometries were observed at high exposure conditions. Specifically, highly crosslinked regions exhibited slight lateral

expansion beyond the intended boundaries. This effect is likely attributable to light scattering and secondary photopolymerization outside the projected region, resulting in localized overcuring.

Another limitation of the present study is that the multimaterial printing workflow was primarily validated using PEGDA formulations containing different dyes to facilitate visualization and quantitative assessment of cross-contamination. While this approach enabled systematic evaluation of the automated vat-switching mechanism and contamination-mitigation strategies, it does not fully capture the challenges associated with printing chemically distinct biomaterial systems. Different photocrosslinkable bioinks can exhibit substantial variations in rheological properties, photopolymerization kinetics, swelling behavior, and interfacial adhesion, which may influence printing fidelity and material integration. Therefore, future studies should investigate the performance of the platform using multiple hydrogel formulations with distinct chemical compositions and biological functionalities.

The current study also primarily focuses on acellular hydrogel fabrication and engineering validation. Although the materials and printing conditions employed are compatible with commonly used photocrosslinkable biomaterials, the effects of multimaterial printing, repeated washing cycles, and variable light exposure on cell viability, proliferation, and long-term function were not investigated. Future work should incorporate cell-laden bioinks and evaluate the biological performance of printed constructs to establish the suitability of the platform for tissue engineering and regenerative medicine applications.

Finally, the open-source nature of the platform provides opportunities for continued community-driven development. Future implementations could incorporate multi-wavelength photopolymerization, volumetric printing strategies, embedded sensing technologies, and organ-on-chip integration. Such advancements may facilitate the fabrication of increasingly sophisticated tissue models and microphysiological systems for applications in tissue engineering, disease modeling, drug discovery, and emerging NAMs.

CONCLUSION

In this work, we developed an open-source multi-vat DLP bioprinting platform that combines automated multimaterial fabrication, programmable stiffness patterning, and high-resolution printing within a low-cost and customizable framework. The system was constructed using commercially available hardware components, open-source electronics, and custom-developed software, providing a reproducible alternative to proprietary DLP printing platforms. The automated rotary vat-switching mechanism enabled the fabrication of compositionally heterogeneous constructs, while integrated washing and drying steps significantly reduced cross-contamination during material transitions. Furthermore, the platform demonstrated the ability to fabricate complex hydrogel architectures with layer thicknesses as low as 5 μm and generate mechanically heterogeneous constructs through spatial control of light exposure, achieving compressive moduli ranging from approximately 50 to 200 kPa using a single bioink formulation. The successful fabrication of vascular networks, anatomical models, multimaterial structures, and stiffness-gradient constructs highlights the versatility of the platform for advanced biofabrication applications. Collectively, this work provides an accessible and fully documented DLP bioprinting platform that lowers barriers to entry for multimaterial biofabrication and offers new opportunities for engineering compositionally and mechanically complex tissue-mimetic constructs.

Acknowledgements

The authors acknowledge financial support from the National Institutes of Health (R01 DE032031). The authors also acknowledge the use of artificial intelligence-assisted tools for language editing. Figures

were prepared by authors using Adobe Illustrator, and selected icons/schematic elements were created or adapted using BioRender. All outputs were reviewed, revised, and validated by the authors, who take full responsibility for the final content of the manuscript.

Author contributions

Syed Raza ur Rehman and Gene Tyler Felix contributed equally to this work and co-developed the open-source multi-vat DLP bioprinting platform under the mentorship of Dr. Akhilesh K. Gaharwar. Gene Tyler Felix led device fabrication, hardware integration, and system assembly, and generated Figures 1-3, Figure S1, and Table S1. Syed Raza ur Rehman led multimaterial printing optimization, construct fabrication, and platform validation, and generated Figures 4-6 and Figure S2. Both authors contributed to device development, printing optimization, data analysis, and manuscript preparation. Yuang Zhang performed the compressive modulus experiments.

Conflict of Interest

The authors declare no conflict of interest.

Data availibility

The data supporting the findings of this study are available on Zenodo at 10.5281/zenodo.XXXXXXXX

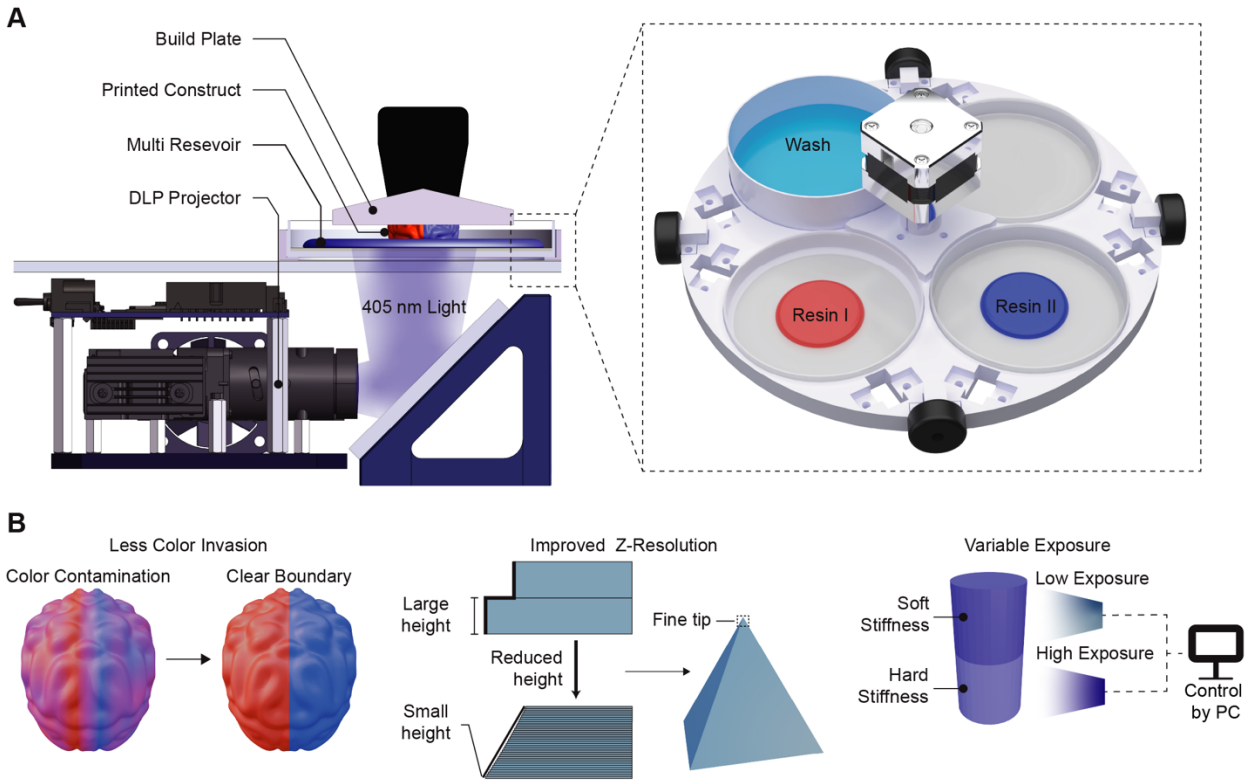

Figure 1. Overview of the open-source multi-vat DLP bioprinting platform.
(A) Schematic of the custom-built DLP bioprinter showing the projection system, build platform, and automated rotary multi-vat mechanism for multimaterial fabrication.
(B) Illustration of the three key capabilities of the platform: reduced cross-contamination during material switching, enhanced z-axis resolution through adjustable layer thickness, and programmable stiffness patterning through variable light exposure.

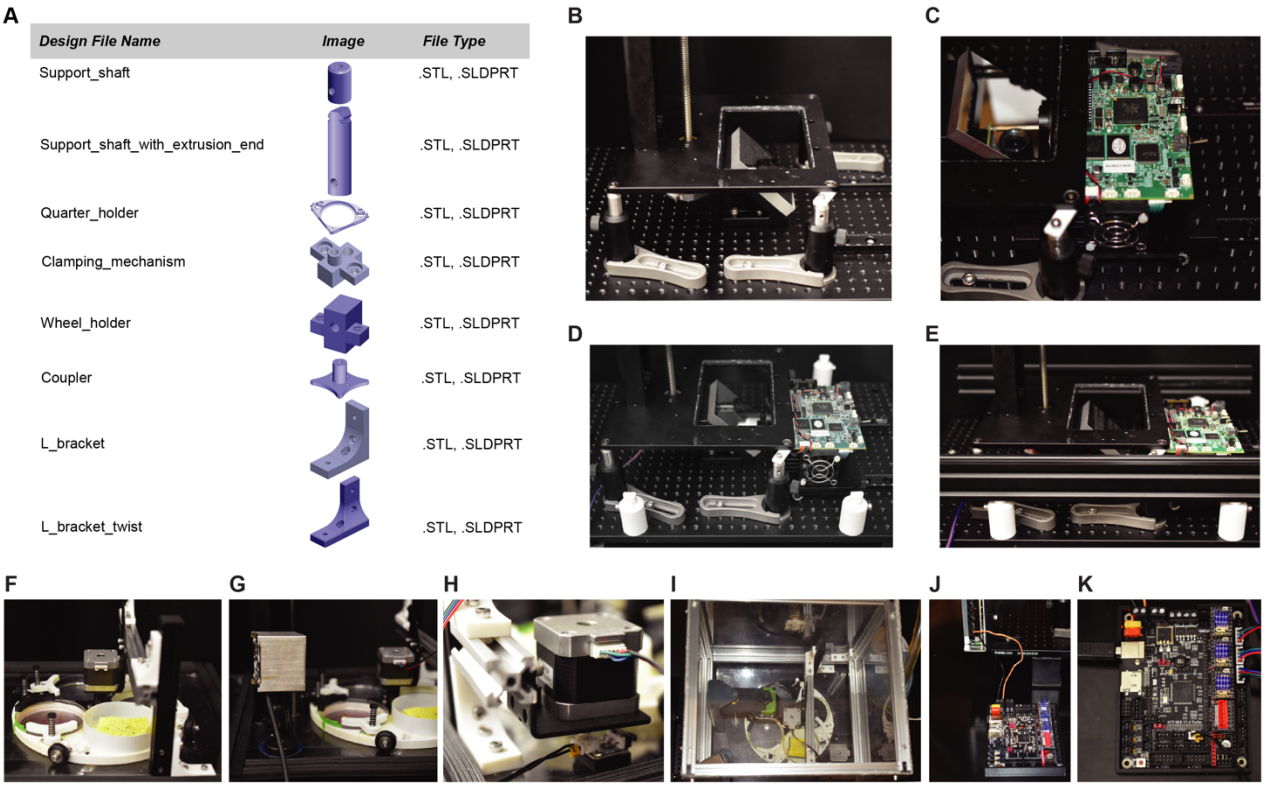

Figure 2. Assembly of the optical and mechanical subsystems of the open-source multi-vat DLP bioprinter.
(A) Exploded view of custom-designed components used for system assembly.
(B) Integration of the projection platform, mirror assembly, and vertical motion system onto the optical breadboard.
(C) Mounting and alignment of the DLP projector using optical rails and dovetail carriers.
(D) Installation of custom 3D-printed supports for structural reinforcement.
(E) Alignment of the projection system using adjustable extrusion-based mounting components.
(F) Rotary multi-vat carousel mounted on a transparent acrylic platform.
(G) Side-mounted air heater for temperature regulation during printing.
(H) Stepper motor-driven locking mechanism for accurate carousel positioning.
(I) Top view of the enclosed printing system integrated with a humidification unit.
(J) SKR V1.4 Turbo controller board and power supply assembly.
(K) Close-up of the SKR V1.4 Turbo showing TMC2209 stepper motor drivers and wiring connections.

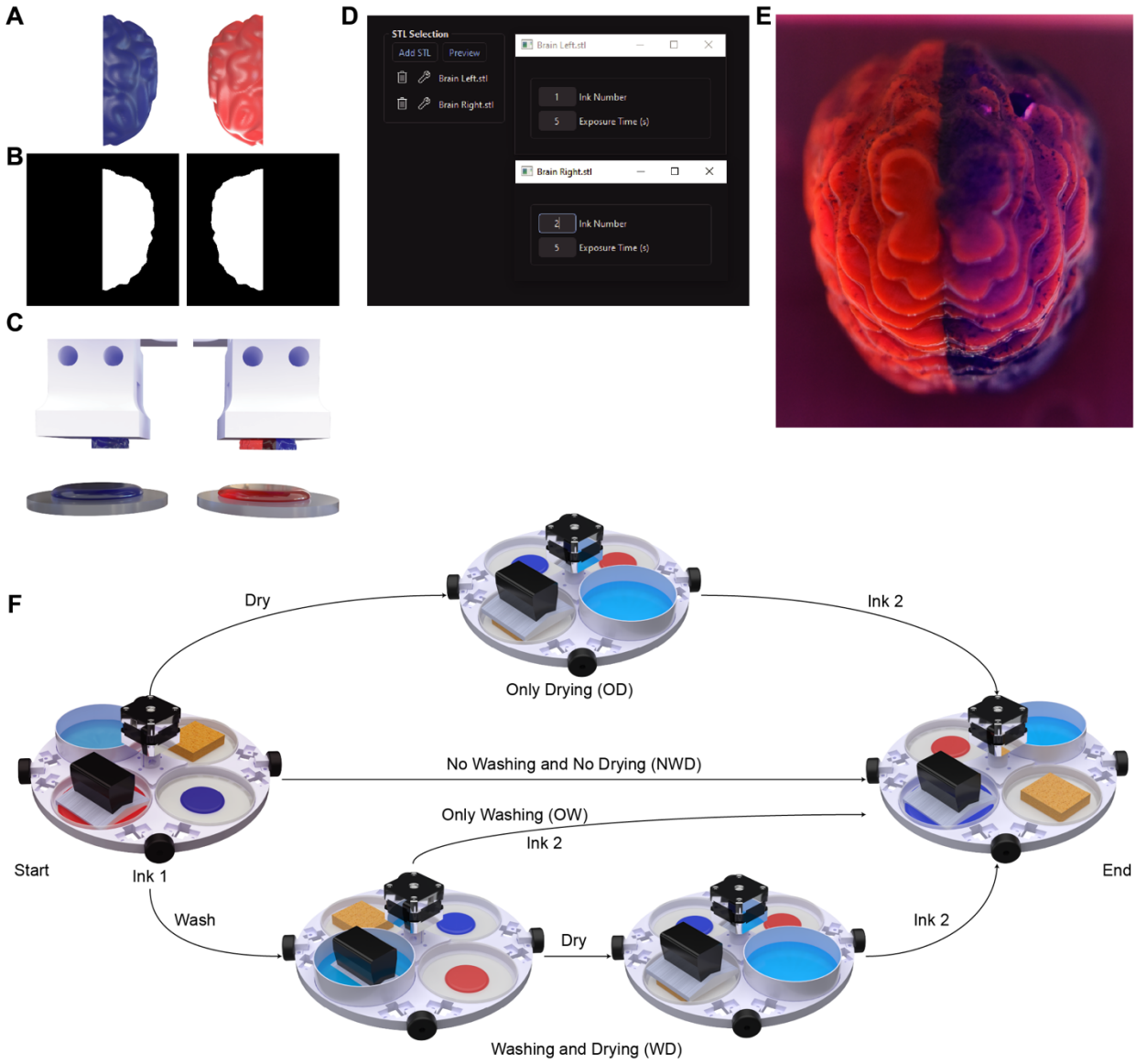

Figure 3. Workflow for automated multimaterial DLP printing.
(A) Separate STL files representing distinct material regions.
(B) Corresponding projected bitmap slices.
(C) Sequential fabrication strategy enabled by automated vat switching.
(D) Custom user interface for assigning material sequence and exposure conditions.
(E) Fabricated multimaterial brain model.
(F) Cleaning and drying workflow used to minimize cross-contamination between resin vats.

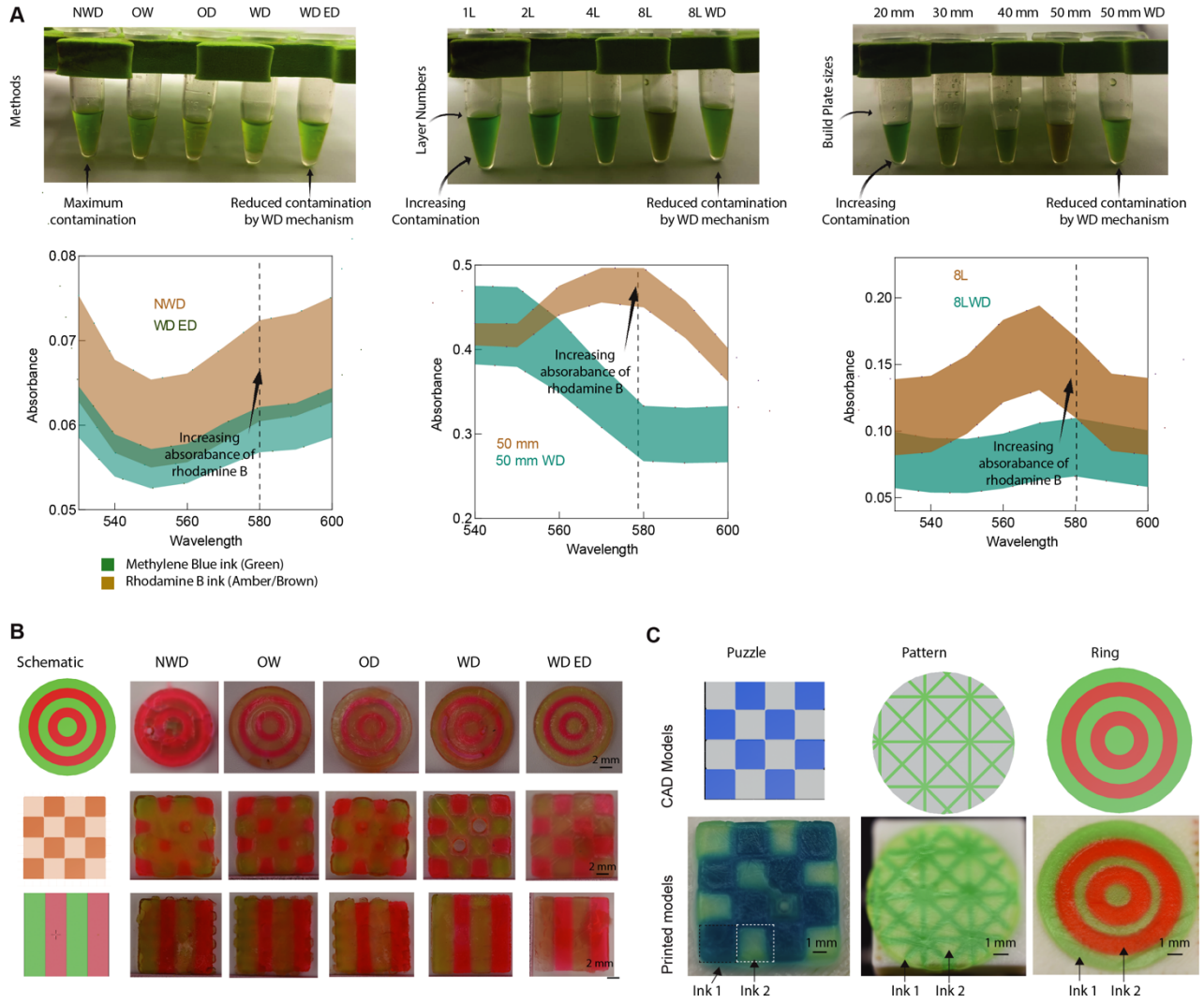

Figure 4. Optimization of multimaterial printing through cross-contamination mitigation.
(A) UV-visible spectroscopy analysis of recovered resin samples showing the effects of cleaning strategy, printed layer number, and build plate size on Rhodamine B carryover. NWD - no washing/no drying, OW - only washing, OD - only drying, WD - washing and drying, and WD+ ED – washing drying with extra dipping cycles.
(B) Comparison of ring, puzzle, and line models fabricated using NWD, OW, OD, WD, and WD+ED workflows.
(C) Representative multimaterial constructs fabricated using the optimized protocol, exhibiting improved interface fidelity and minimal cross-contamination.

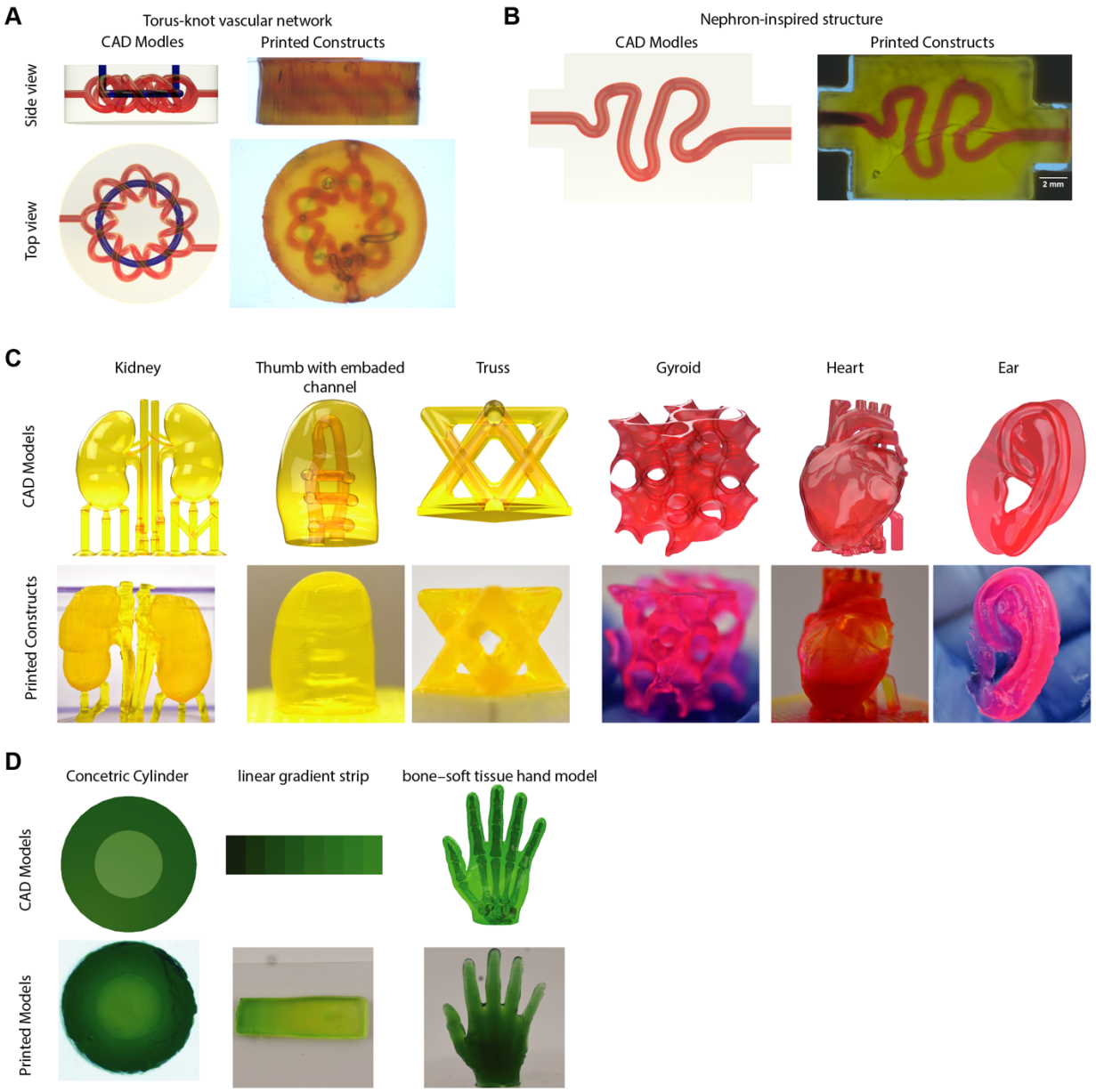

Figure 5. High-resolution fabrication and patterning of hydrogel architectures.
(A) CAD model and printed torus-knot vascular network demonstrating the ability to fabricate complex interconnected channel geometries.
(B) CAD model and printed nephron-inspired structure containing embedded vascular channels with a diameter of approximately 1 mm.
(C) CAD models and corresponding printed constructs, including kidneys, thumb with embedded channel, truss, gyroid, heart, and ear structures.
(D) Representative stiffness-patterned constructs fabricated by varying light exposure, including a concentric cylinder, linear gradient strip, and bone–soft tissue hand model.

Table 1. Custom design files summary.

Part Name	Model Name	Cost	Quantity	Availability	URL Link
Resin Printer	Photon Ultra	$600	1	No	https://store.anycubic.com/products/photon-ultra
Resin Printer (alternative)	Photon Mono 4 Ultra	$314.49	1	Yes	https://www.amazon.com/ANYCUBIC-Mono-Ultra-Intelligent-6-04x3-42x/dp/B0DB88XY7X
Thermoplastic Printer	Ender 3 Pro		1	No	
Thermoplastic Printer (alternative)	Ender 3	$175.99	1	Yes	https://www.amazon.com/Comgrow-Creality-Ender-Aluminum-220x220x250mm/dp/B07BR3F9N6
Motor Controller + Motor Drivers	SKR V1.4 Turbo + TMC 2209	$65.99	1	Yes	https://www.amazon.com/BIGTREETECH-Controller-Compatible-With12864LCD-5TMC2209/dp/B082QYYFVX
Magnetic Build Plate		$18.99	1	Yes	https://www.amazon.com/KOYOFEI-Anycubic-Flexible-Magnetic-Platform/dp/B0DQ59CJDY
Breadboard	MS12B/M	$334.31	1	Yes	https://www.thorlabs.com/item/MS12B_M
Post Holders	PH2-P5	$45.66	1	Yes	https://www.thorlabs.com/item/PH2-P5#ad-image-0
Rail	RLA 150/M	$53.69	2	Yes	https://www.thorlabs.com/item/RLA150_M
Mirror Holder	AP45/M	$99.16	1	Yes	https://www.thorlabs.com/item/AP45_M
Clamping Forks	CF125-P5	$49.12	1	Yes	https://www.thorlabs.com/item/CF125-P5
Rail Carrier	RC2/M	$36.56	4	Yes	https://www.thorlabs.com/item/RC2_M
Optical Posts	TR1.5	$6.05	4	Yes	https://www.thorlabs.com/item/TR1.5
DLP Projector (alternative)	E4500 Mk I UVGB		1	No	https://www.ekbtechnologies.com/e-store/dlp-lightcrafter-e4500-mkii-uv-385nm-405nm-blue-460nm-green-520nm-on-axis?c=5cb86ca038d9a
DLP Projector	E4500 Mk II	$1619.00	1	Yes	https://www.ekbtechnologies.com/e-store/lightcrafter-e4500mkii-plus-2w-uv?c=5cb86ca432c93
Optical Mirror	Aluminum Mirror	$260.00	1	Yes	https://www.edmundoptics.com/p/75-x-75mm-uv-enhanced-aluminum-lambda4-mirror/5810/
Power Supply	LRS 350-24	$127.52	1	Yes	https://www.amazon.com/LRS-350-24-Switching-Supply-350-4W-115Vac/dp/B072FNHWPL?th=1
Thermoplastic Printer	Ender 3	$179.00	1	Yes	https://www.amazon.com/Comgrow-Creality-Ender-Aluminum-220x220x250mm/dp/B07BR3F9N6
Acrylic Sheet		$45.98	1	Yes	https://www.homedepot.com/p/OPTIX-24-in-x-48-in-x-0-093-3-32-in-Clear-Acrylic-Sheet-MC-13/202038048?source=shoppingads&locale=en-US&gStoreCode=6559&gQT=1
Thermoplastic Printer	A1 Mini	$219.00	1	Yes	https://us.store.bambulab.com/products/a1-mini
PLA Plastic	PLA Basic	$19.99	1	Yes	https://us.store.bambulab.com/products/pla-basic-filament
Enclosure Panel Kit	V-Core 3	$509	1	Yes	https://clearviewplastic.com/products/ratrig-vcore-3-panel-kit-for-300mm-400mm-500mm
Air Heater	H1		1	No	Not available
Air Heater	H2	$51.99	1	Yes	https://www.chitusystems.com/products/3d-printer-heater?variant=46074147635436
Humidifier	HM500TG		1	No	https://www.ebay.com/itm/184929182033

REFERENCES:

(1) Ashammakhi, N.; Ahadian, S.; Xu, C.; Montazerian, H.; Ko, H.; Nasiri, R.; Barros, N.; Khademhosseini, A. Bioinks and bioprinting technologies to make heterogeneous and biomimetic tissue constructs. *Materials Today Bio* **2019**, *1*, 100008.
(2) Hua, W.; Gaharwar, A. K. 3D biofabricated in vitro models as new approach methodologies for animal alternatives. *npj Biomedical Innovations* **2026**, *3* (1), 20.
(3) Wistner, S. C.; Rashad, L.; Slaughter, G. Advances in tissue engineering and biofabrication for in vitro skin modeling. *Bioprinting* **2023**, *35*, e00306.
(4) Chen, A.; Wang, W.; Mao, Z.; He, Y.; Chen, S.; Liu, G.; Su, J.; Feng, P.; Shi, Y.; Yan, C. Multimaterial 3D and 4D bioprinting of heterogenous constructs for tissue engineering. *Advanced Materials* **2024**, *36* (34), 2307686.
(5) Liu, W.; Zhang, Y. S.; Heinrich, M. A.; De Ferrari, F.; Jang, H. L.; Bakht, S. M.; Alvarez, M. M.; Yang, J.; Li, Y. C.; Trujillo-de Santiago, G. Rapid continuous multimaterial extrusion bioprinting. *Advanced materials* **2017**, *29* (3), 1604630.
(6) Chimene, D.; Peak, C. W.; Gentry, J. L.; Carrow, J. K.; Cross, L. M.; Mondragon, E.; Cardoso, G. B.; Kaunas, R.; Gaharwar, A. K. Nanoengineered ionic–covalent entanglement (NICE) bioinks for 3D bioprinting. *ACS applied materials & interfaces* **2018**, *10* (12), 9957–9968.
(7) Chimene, D.; Deo, K. A.; Thomas, J.; Dahle, L.; Mandrona, C.; Gaharwar, A. K. Designing cost-effective open-source multihead 3D bioprinters. *GEN biotechnology* **2022**, *1* (4), 386–400.
(8) Compaan, A. M.; Christensen, K.; Huang, Y. Inkjet bioprinting of 3D silk fibroin cellular constructs using sacrificial alginate. *ACS Biomaterials Science & Engineering* **2017**, *3* (8), 1519–1526.
(9) Rayner, S. G.; Howard, C. C.; Mandrycky, C. J.; Stamenkovic, S.; Himmelfarb, J.; Shih, A. Y.; Zheng, Y. Multiphoton-guided creation of complex organ-specific microvasculature. *Advanced healthcare materials* **2021**, *10* (10), 2100031.
(10) Guillotin, B.; Souquet, A.; Catros, S.; Duocastella, M.; Pippenger, B.; Bellance, S.; Bareille, R.; Rémy, M.; Bordenave, L.; Amédée, J. Laser assisted bioprinting of engineered tissue with high cell density and microscale organization. *Biomaterials* **2010**, *31* (28), 7250–7256.
(11) Florczak, S.; Größbacher, G.; Ribezzi, D.; Longoni, A.; Gueye, M.; Grandidier, E.; Malda, J.; Levato, R. Adaptive and context-aware volumetric printing. *Nature* **2025**, *645* (8079), 108–114.
(12) Grigoryan, B.; Paulsen, S. J.; Corbett, D. C.; Sazer, D. W.; Fortin, C. L.; Zaita, A. J.; Greenfield, P. T.; Calafat, N. J.; Gounley, J. P.; Ta, A. H. Multivascular networks and functional intravascular topologies within biocompatible hydrogels. *Science* **2019**, *364* (6439), 458–464.
(13) Bhusal, A.; Dogan, E.; Nguyen, H.-A.; Labutina, O.; Nieto, D.; Khademhosseini, A.; Miri, A. K. Multi-material digital light processing bioprinting of hydrogel-based microfluidic chips. *Biofabrication* **2022**, *14* (1), 014103.
(14) Wang, M.; Li, W.; Mille, L. S.; Ching, T.; Luo, Z.; Tang, G.; Garciamendez, C. E.; Lesha, A.; Hashimoto, M.; Zhang, Y. S. Digital light processing based bioprinting with composable gradients. *Advanced Materials* **2022**, *34* (1), 2107038.
(15) Yang, M.; Chu, L.; Zhuang, Y.; Qi, C.; Meng, S.; Liu, Z.; Kong, T. Multi-material digital light processing (DLP) bioprinting of heterogeneous hydrogel constructs with perfusable networks. *Advanced functional materials* **2024**, *34* (32), 2316456.

(16) Zhang, Y.; Davis Jr, R.; Biswas, S.; Miller, S. E.; Raza Ur Rehman, S.; Felix, G. T.; Gaharwar, A. K. Multiscale Engineered Heterogeneous Hydrogel Composites for Digital Light Processing 3D Printing. *ACS Applied Materials & Interfaces* **2025**, *17* (37), 51605–51619.
(17) Ravanbakhsh, H.; Karamzadeh, V.; Bao, G.; Mongeau, L.; Juncker, D.; Zhang, Y. S. Emerging technologies in multi-material bioprinting. *Advanced Materials* **2021**, *33* (49), 2104730.
(18) Wang, M.; Li, W.; Hao, J.; Gonzales III, A.; Zhao, Z.; Flores, R. S.; Kuang, X.; Mu, X.; Ching, T.; Tang, G. Molecularly cleavable bioinks facilitate high-performance digital light processing-based bioprinting of functional volumetric soft tissues. *Nature communications* **2022**, *13* (1), 3317.
(19) Wang, Z.; Abdulla, R.; Parker, B.; Samanipour, R.; Ghosh, S.; Kim, K. A simple and high-resolution stereolithography-based 3D bioprinting system using visible light crosslinkable bioinks. *Biofabrication* **2015**, *7* (4), 045009.
(20) Kuang, X.; Wu, J.; Chen, K.; Zhao, Z.; Ding, Z.; Hu, F.; Fang, D.; Qi, H. J. Grayscale digital light processing 3D printing for highly functionally graded materials. *Science advances* **2019**, *5* (5), eaav5790.
(21) Crosby, C. O. Open-source extrusion 3D bioprinters: Trends and recommendations. *Bioprinting* **2024**, *38*, e00336.
(22) Sanchez-Garcia, D.; Giménez-El-Amrani, A.; Gonzalez-Muñoz, A.; Sanz-Garcia, A. An Open-Source 3D Bioprinter Using Direct Light Processing for Tissue Engineering Applications. *Inventions* **2025**, *10* (5), 92.
(23) Cheng, J.; Yu, S.; Wang, R.; Ge, Q. Digital light processing based multimaterial 3D printing: challenges, solutions and perspectives. *International Journal of Extreme Manufacturing* **2024**, *6* (4), 042006.
(24) Bernal, P. N.; Delrot, P.; Loterie, D.; Li, Y.; Malda, J.; Moser, C.; Levato, R. Volumetric bioprinting of complex living-tissue constructs within seconds. *Advanced materials* **2019**, *31* (42), 1904209.
(25) Lu, Z.; Gao, W.; Liu, F.; Cui, J.; Feng, S.; Liang, C.; Guo, Y.; Wang, Z.; Mao, Z.; Zhang, B. Vat photopolymerization based digital light processing 3D printing hydrogels in biomedical fields: Key parameters and perspective. *Additive Manufacturing* **2024**, *94*, 104443.
(26) Zhu, M.; Tao, H.; Samani, M.; Luo, M.; Wang, X.; Hopyan, S.; Sun, Y. Spatial mapping of tissue properties in vivo reveals a 3D stiffness gradient in the mouse limb bud. *Proceedings of the National Academy of Sciences* **2020**, *117* (9), 4781–4791.

Supplementary Information

Designing an Open-Source Multi-vat Digital Light Processing Printer

Syed Raza ur Rehman [#1], Gene Tyler Felix [#1], Yuang Zhang[1], Akhilesh K Gaharwar[1,2,3]*

[1]Department of Biomedical Engineering, College of Engineering, Texas A&M University, College Station, TX 77843, USA
[2]Department of Material Science and Engineering, College of Engineering, Texas A&M University, College Station, TX 77843, USA
[3]Interdisiplinary program in Genetics and Genomics, Texas A&M University, College Station, TX 77843, USA
*Corresponding author E-mail: gaharwar@tamu.edu (A.K.G.)
[#]Equal contribution

Keywords: Digital Light Processing; Open Source; Multi-material; Additive Manufacturing

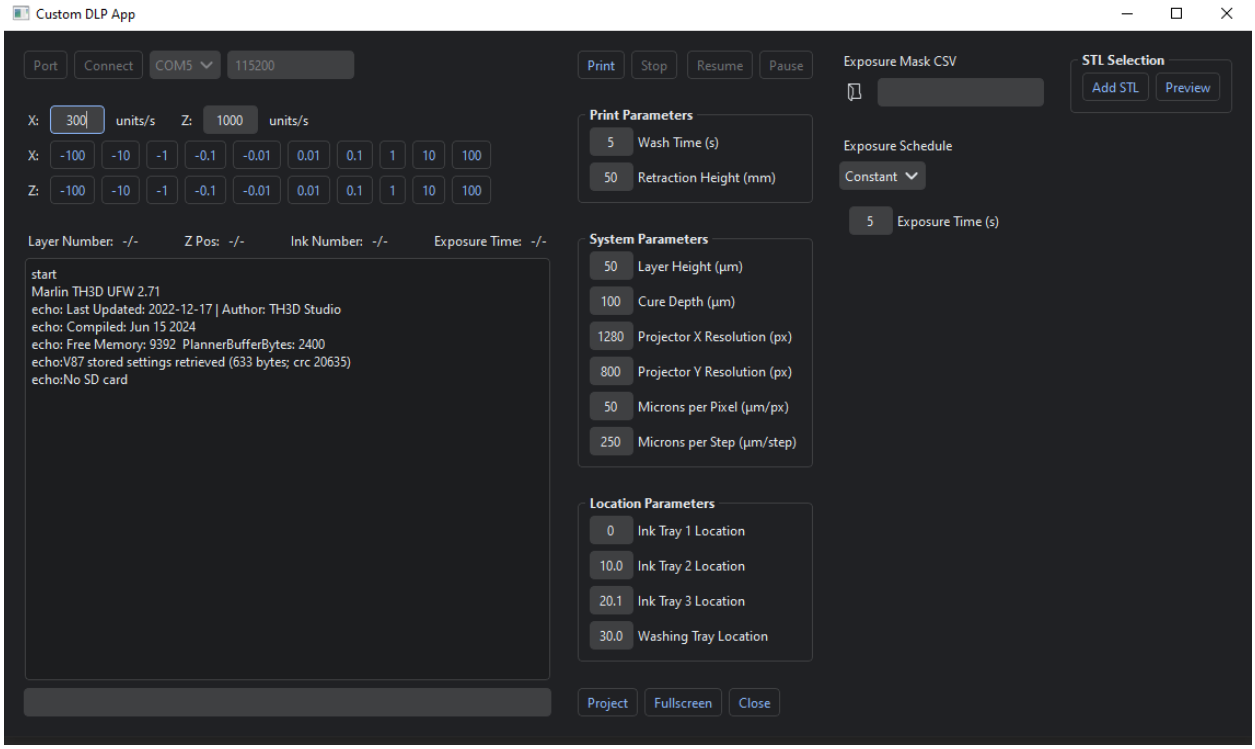

Figure S1: Python-based graphical user interface.

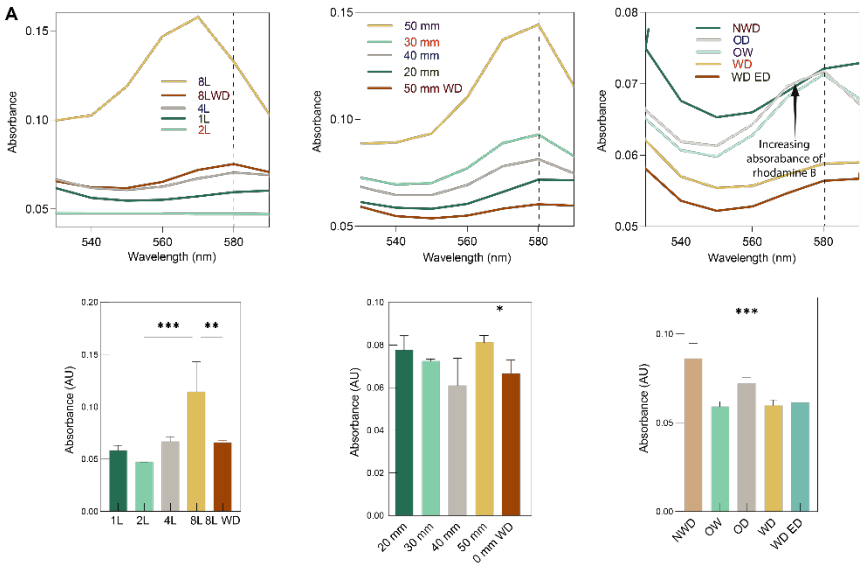

Figure S2. Optimization of multimaterial printing through cross-contamination mitigation. (A) UV–visible spectroscopy analysis of recovered resin samples showing the effects of cleaning strategy, printed layer number, and build plate size on Rhodamine B carryover.